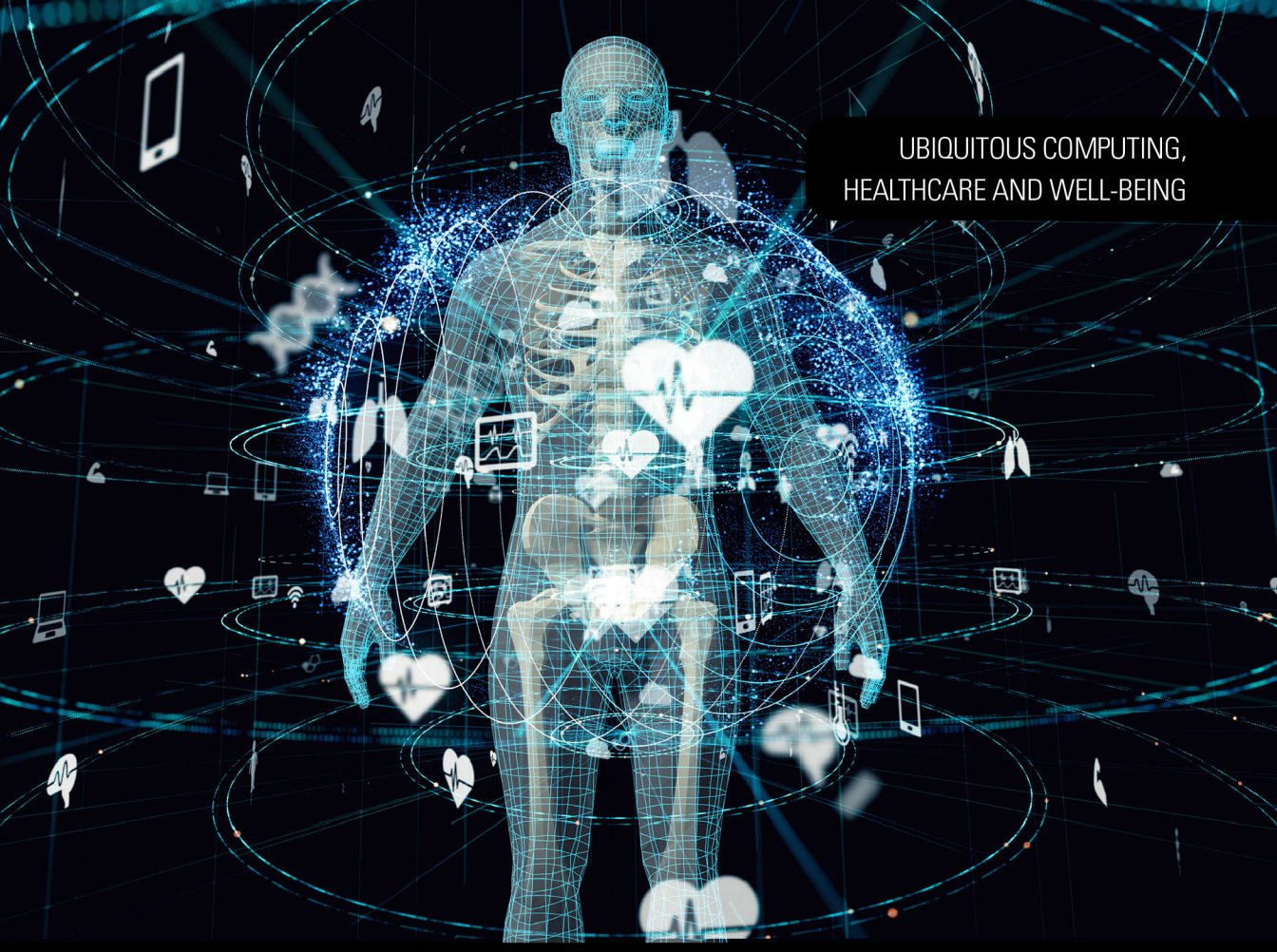


# Human Activity and Behavior Analysis

## Advances in Computer Vision and Sensors

Volume 1

**Edited by**

**Md Atiqur Rahman Ahad**
**Sozo Inoue**
**Guillaume Lopez**
**Tahera Hossain**

CRC Press
Taylor & Francis Group

# *Human Activity and Behavior Analysis*

Human Activity and Behavior Analysis relates to the field of vision and sensor-based human action or activity and behavior analysis and recognition. The book includes a series of methodologies, surveys, relevant datasets, challenging applications, ideas, and future prospects.

The book discusses topics such as action recognition, action understanding, gait analysis, gesture recognition, behavior analysis, emotion and affective computing, and related areas. This volume focuses on two relevant activities in three main subject areas: Healthcare and Emotion, Mental Health, and Nurse Care Records.

The editors are experts in these arenas and the contributing authors are drawn from high-impact research groups around the world. This book will be of great interest to academics, students, and professionals working and researching in the field of human activity and behavior analysis.

## Ubiquitous Computing, Healthcare and Well-being

Human Activity Recognition has been researched in thousands of papers, with mobile/environmental sensors in ubiquitous/pervasive domains, and with cameras in vision domains. Human Behavior Analysis is also explored for long-term health care, rehabilitation, emotion recognition, human interaction, and so on. However, many research challenges remain for realistic settings, such as complex and ambiguous activities/behavior, optimal sensor combinations, (deep) machine learning, data collection, platform systems, and applications.

The ***Ubiquitous Computing, Healthcare and Well-being*** Series provides a forum for capturing the latest advances and setting the course for future research in these areas. Books in the series will typically be presented by leading researchers globally and will cover, among other things: original methods; exploration of new applications; excellent survey papers; presentations on relevant datasets; challenging applications; ideas and future scopes; guidelines.

*Series Editors:*
***Sozo Inoue**, Professor and Director of the Care XDX Center, Kyushu Institute of Technology, Japan*
***Md Atiqur Rahman Ahad**, Associate Professor of Artificial Intelligence and Machine Learning, Department of Computer Science and Digital Technology, University of East London, UK*

**Human Activity and Behavior Analysis: Advances in Computer Vision and Sensors: Volume 1**
*Edited by Md Atiqur Rahman Ahad, Sozo Inoue, Guillaume Lopez, Tahera Hossain*

**Human Activity and Behavior Analysis: Advances in Computer Vision and Sensors: Volume 2**
*Edited by Md Atiqur Rahman Ahad, Sozo Inoue, Guillaume Lopez, Tahera Hossain*

For more information about this series please visit:
https://www.routledge.com/UbiquitousComputingHealthcareandWell-being/book-series/UCHAWB

# *Human Activity and Behavior Analysis*

## Advances in Computer Vision and Sensors: Volume 1

Edited by

Md Atiqur Rahman Ahad, Sozo Inoue,
Guillaume Lopez, and Tahera Hossain

CRC Press
Taylor & Francis Group
Boca Raton London New York

CRC Press is an imprint of the
Taylor & Francis Group, an **informa** business

Designed cover image: Shutterstock

First edition published 2024
by CRC Press
6000 Broken Sound Parkway NW, Suite 300, Boca Raton, FL 33487-2742

and by CRC Press
4 Park Square, Milton Park, Abingdon, Oxon, OX14 4RN

*CRC Press is an imprint of Taylor & Francis Group, LLC*



ISBN: 9781032443119 (hbk)
ISBN: 9781032430812 (pbk)
ISBN: 9781003371540 (ebk)

DOI: 10.1201/9781003371540

Typeset in Minion
by codeMantra

# Contents

PART III Nurse Care Records

# Preface

Sensors and cameras are exploited for the analysis and recognition of human activity and behavior. In the book *Human Activity and Behavior Analysis: Advances in Computer Vision and Sensors*, we have divided across two volumes, 40 wonderful chapters under five parts: Part 1: Healthcare and Emotion (Chapters 1–7), Part 2: Mental Health (Chapters 8–14), Part 3: Nurse Care Records (Chapters 15–26), Part 4: Movement and Sensors (Chapters 27–36), and Part 5: Sports Activity Analysis (Chapters 37–40). These chapters were developed from the *Fourth International Conference on Activity and Behavior Computing* (ABC 2022, https://abc-research.github.io/), held at University of East London, UK. These chapters were selected after a rigorous review process by related top experts, and strict review rebuttal process. We believe the chapters will enrich the research community in the field of *Activity and Behavior Computing (ABC)*. We hope that this book will ignite several exciting research directions. We cordially thank all authors, reviewers, and chairs for their great efforts.

**Best regards**,

Md Atiqur Rahman Ahad, *University of East London, UK*
Sozo Inoue, *Kyushu Institute of Technology, Japan*
Guillaume Lopez, *Aoyama Gakuin University, Japan*
Tahera Hossain, *Aoyama Gakuin University, Japan*

# Editors

**Md Atiqur Rahman Ahad**, PhD, is Associate Professor of AI and M at the University of East London, UK.

**Sozo Inoue**, PhD, is Professor at the Kyushu Institute of Technology, Japan.

**Guillaume Lopez**, PhD, is Professor at Aoyama Gakuin University, Japan.

**Tahera Hossain**, PhD, is Assistant Professor (Project) at Aoyama Gakuin University, Japan.

# Contributors

**Nouran Abdalazim**
Faculty of Informatics
Università della Svizzera Italiana (USI)
Lugano, Switzerland

**Md. Akhtaruzzaman Adnan**
Department of Computer Science and Engineering
University of Asia Pacific
Dhaka, Bangladesh

**Md Atiqur Rahman Ahad**
Department of Computer Science & Digital Technology
University of East London
London, UK

**Wasim Akram**
Department of Computer Sicence and Engineering
East West University
Dhaka, Bangladesh

**Sumya Akter**
Department of Computer Science and Engineering
University of Asia Pacific
Dhaka, Bangladesh

**Leonardo Alchieri**
Faculty of Informatics
Università della Svizzera Italiana (USI)
Lugano, Switzerland

**Lidia Alecci**
Faculty of Informatics
Università della Svizzera Italiana (USI)
Lugano, Switzerland

**Sayeda Shamma Alia**
Department of Life Science and System Engineering
Kyushu Institute of Technology
Kitakyushu, Japan

**R. Askari**
Department of Chemical and Biological Engineering
Illinois Institute of Technology
Chicago, Illinois

**A. Cinar**
Department of Chemical and Biological Engineering
Department of Biomedical Engineering
Illinois Institute of Technology
Chicago, Illinois

**Ian Cleland**
School of Computing
Ulster University
Northern Ireland, United Kingdom

**Zachary Dair**
Department of Computer Science
Munster Technological University
Cork, Ireland

**Pritom Debnath**
American International University-Bangladesh
Dhaka, Bangladesh

**Samantha Dockray**
Department of Applied Psychology
University College Cork
Cork, Ireland

**Gulustan Dogan**
Department of Computer Science
University of North Carolina
Wilmington, USA

**Muhammad Fikry**
Department of Life Science and System Engineering
Graduate School of Life Science and Systems Engineering
Kyushu Institute of Technology
Kitakyushu, Japan
and
Universitas Malikussaleh
Lhokseumawe, Indonesia

**Björn Friedrich**
Department of Health Services Research
Carl von Ossietzky University
Oldenburg, Germany

**Kensi Fujiwara**
Department of Computer Science and Engineering
Toyohashi University of Technology
Toyohashi, Japan

**Christina Garcia**
Department of Life Science and Systems Engineering
Kyushu Institute of Technology
Kitakyushu, Japan

**Shkurta Gashi**
Faculty of Informatics
Università della Svizzera Italiana (USI)
Lugano, Switzerland

**Cappon Giacomo**
Department of Information Engineering
University of Padova
Padova, Italy

**Nuno Gomes**
The Instituto Superior de Engenharia de Lisboa
Instituto Politécnico de Lisboa
Lisboa, Portugal

**Defry Hamdhana**
Department of Life Science and System Engineering
Kyushu Institute of Technology
Kitakyushu, Japan

**Andreas Hein**
OFFIS R+D Division Health, Escherweg
Oldenburg, Germany

**John Hendricks**
Department of Computer Science
University of North Carolina
Wilmington, USA

**Kazuki Honda**
Graduate School of Science and Engineering
Aoyama Gakuin University
Tokyo, Japan

**Shahera Hossain**
Department of Computer Science and Engineering
University of Asia Pacific
Dhaka, Bangladesh

**Tahera Hossain**
Graduate School of Science and Engineering
Aoyama Gakuin University
Tokyo, Japan

**Yoshinori Ideno**
Nagoya University
Nagoya, Japan
and
Global Business Division
Carecom Co., Ltd
Tokyo, Japan

**Sozo Inoue**
Department of Life Science and Systems Engineering
Kyushu Institute of Technology
Kitakyushu, Japan

**Mohammad Sabik Irbaz**
Department of Computer Science and Engineering
Islamic University of Technology
Gazipur City, Bangladesh

**Naoko Ishibashi**
Department of Child Development
Sugiyama Jogakuen University
Nagoya, Japan

**Naoya Isoyama**
Department of Information Science
Nara Institute of Science and Technology
Ikoma, Japan

**Miyuki Iwamoto**
Department of Advanced Fibro-Science
Kyoto Institute of Technology
Kyoto, Japan

**Md. Kabiruzzaman**
Department of Electrical and Electronic Engineering
American International University-Bangladesh
Dhaka, Bangladesh

**Rashid Kamal**
School of Computing
Ulster University
Northern Ireland, United Kingdom

**Haru Kaneko**
Department of Life Science and Systems Engineering
Kyushu Institute of Technology
Kitakyushu, Japan

**Yusuke Kawasaki**
Graduate School of Science and Engineering
Aoyama Gakuin University
Tokyo, Japan

**Maryam Khalid**
Department of Electrical Computer Engineering
Rice University
Houston, Texas

**Kiyoshi Kiyokawa**
Department of Information Science
Nara Institute of Science and Technology
Ikoma, Japan

**Huakun Liu**
Department of Information Science
Nara Institute of Science and Technology
Ikoma, Japan

**Guillaume Lopez**
College of Science and Engineering
Department of Integrated Information Technology
Aoyama Gakuin University
Tokyo, Japan

**Lutfun Nahar Lota**
Department of Computer Science and Engineering
Islamic University of Technology
Gazipur City, Bangladesh

**Andrè Lourenço**
Instituto Superior de Engenharia de Lisboa
Instituto Politécnico de Lisboa
Lisboa, Portugal
and
CardioID Technologies
Lisboa, Portugal

**Cossu Luca**
Department of Information Engineering
University of Padova
Padova, Italy

**Vettoretti Martina**
Department of Information Engineering
University of Padova
Padova, Italy

**Paul McCullagh**
School of Computing
Ulster University
Northern Ireland, United Kingdom

**Atzeni Michele**
Department of Information Engineering
University of Padova
Padova, Italy

**Nazmun Nahid**
Department of Life Science and System Engineering
Kyushu Institute of Technology
Kitakyushu, Japan

**Atsushi Nakazawa**
Graduate School of Interdisciplinary Science and Engineering in Health Systems
Okayama University
Kyoto, Japan

**Kizito Nkurikiyeyezu**
Graduate School of Science and Engineering
Aoyama Gakuin University
Tokyo, Japan

**Chris Nugent**
School of Computing
Ulster University
Northern Ireland, United Kingdom

**Ruairi O'Reilly**
Department of computer science
Munster Technological University
Cork, Ireland

**Ren Ohmura**
Department of Computer Science and Engineering
Toyohashi University of Technology
Toyohashi, Japan

**Akira Omi**
Department of Computer Science and Engineering
Toyohashi University of Technology
Toyohashi, Japan

**Shintaro Oyama**
Department of Hand Surgery
Hospital Medical IT Center
Nagoya University
Nagoya, Japan

**Matilde Pato**
Instituto Superior de Engenharia de Lisboa
Instituto Politécnico de Lisboa and LASIGE, FCUL
Universidade de Lisboa
Lisboa, Portugal

**Urja Pawar**
Department of Computer Science
Munster Technological University
Cork, Ireland

**Monica Perusquía-Hernández**
Department of Information Science
Nara Institute of Science and Technology
Ikoma, Japan

**Tanmoy Sarkar Pias**
Department of Computer Science
Virginia Tech
Blacksburg, Virginia

**Yeasin Arafat Pritom**
Department of Electrical and Electronic Engineering
University of Dhaka
Dhaka, Bangladesh

**Rumman Ahmed Prodhan**
Department of Computer Science and Engineering
University of Asia Pacific
Dhaka, Bangladesh

**L. Quinn**
Department of Biobehavioral Nursing Science
University of Illinois
Chicago, Illinois

**Vu Nguyen Phuong Quynh**
Department of Life Science and System Engineering
Graduate School of Life Science and Systems Engineering
Kyushu Institute of Technology
Kitakyushu, Japan

**Hasib Ryan Rahman**
Department of Electrical and Electronic Engineering
University of Dhaka
Dhaka, Bangladesh

**Md. Sohanur Rahman**
Department of Electrical and Electronic Engineering
University of Dhaka
Dhaka, Bangladesh

**M. Rashid**
Department of Chemical and Biological Engineering
Illinois Institute of Technology
Chicago, Illinois

**Md. Golam Rasul**
Department of Data Science
Universitat Potsdam
Potsdam, Germany

**Lourenço Rodrigues**
Instituto Superior de Engenharia de Lisboa
Instituto Politécnico de Lisboa
Lisboa, Portugal
and
CardioID Technologies
Lisboa, Portugal

**Muhammad Saad**
Department of Computer Science
Munster Technological University
Cork, Ireland

**Yuji Sakamoto**
Global Business Division
Carecom Co., Ltd
Tokyo, Japan

**Fardin Ahsan Sakib**
Department of Computer Science and Engineering
George Mason University
George Mason, Virginia

**Akane Sano**
Department of Electrical Computer Engineering, Computer Science, and Bioengineering
Rice University
Houston, Texas

**Silvia Santini**
Faculty of Informatics
Università della Svizzera Italiana (USI)
Lugano, Switzerland

**Pedro Santos**
The Instituto Superior de Engenharia de Lisboa
Instituto Politécnico de Lisboa
Lisboa, Portugal

**Tanjila Alam Sathi**
Department of Computer Science and Engineering
Islamic University of Technology
Gazipur City, Bangladesh

**Alicia Choto Segovia**
Department of Electrical Computer Engineering
Rice University
Houston, Texas

**M. Sevil**
Department of Biomedical Engineering
Illinois Institute of Technology
Chicago, Illinois

**L. Sharp**
Department of Pharmacy Systems Outcomes and Policy
University of Illinois Chicago
Chicago, Illinois

**Md. Mamun Sheikh**
Department of Electrical and Electronic Engineering
University of Dhaka
Dhaka, Bangladesh

**Tomohiro Shibata**
Department of Life Science and System Engineering, Graduate School of Life Science and Systems Engineering
Kyushu Institute of Technology
Kitakyushu, Japan

**Yuko Shibata**
Department of Life Science and System Engineering, Graduate School of Life Science and Systems Engineering
Kyushu Institute of Technology
Kitakyushu, Japan

**Mohammad Shidujaman**
Department of Computer Science and Engineering
Independent University
Dhaka, Bangladesh

**Shadril Hassan Shifat**
Department of Computer Science and Engineering
American International University-Bangladesh
Dhaka, Bangladesh

**Riku Shinohara**
Department of Information Science
Nara Institute of Science and Technology
Ikoma, Japan

**Jonathan Sturdivant**
Department of Computer Science
University of North Carolina
Wilmington, USA

**Tomoya Suzuki**
Department of Integrated Information Technology
Aoyama Gakuin University
Tokyo, Japan

**Akihito Taya**
Department of Integrated Information Technology
Aoyama Gakuin University
Tokyo, Japan

**Tahia Tazin**
Department of Human Intelligence Systems
Kyushu Institute of Technology
Kitakyushu, Japan

**Yoshito Tobe**
Department of Integrated Information Technology
Aoyama Gakuin University
Tokyo, Japan

**Masato Uchimura**
Department of Life Science and Systems Engineering
Kyushu Institute of Technology
Kitakyushu, Japan

**Hideaki Uchiyama**
Department of Information Science
Nara Institute of Science and Technology
Ikoma, Japan

**Thomas Vaessen**
Faculty of Behavioural, Management and Social Sciences (BMS), Psychology, Health and Technology (PGT)
University of Twente
Drienerlolaan, Netherlands

**John Noel Victorino**
Department of Life Science and System Engineering, Graduate School of Life Science and Systems Engineering
Kyushu Institute of Technology
Kitakyushu, Japan

**Keiko Yamashita**
Innovative Research Center for Preventive Medical Engineering
Institute of Innovation for Future Society
Nagoya University
Nagoya, Japan

**Huiyuan Yang**
Department of Electrical Computer Engineering
Rice University
Houston, Texas

**Han Yu**
Department of Electrical Computer Engineering
Rice University
Houston, Texas

**Abrar Zarif**
Department of Electrical and Electronic Engineering
University of Dhaka
Dhaka, Bangladesh

**Sayeda Fatema Tuj Zohura**
Department of Computer Sicence and Engineering
East West University
Dhaka, Bangladesh

# I

# Healthcare and Emotion

# Forecasting Parkinson's Disease Patients' Wearing-Off Using Wrist-Worn Fitness Tracker and Smartphone Dataset

**John Noel Victorino, Yuko Shibata, Sozo Inoue, and Tomohiro Shibata**

*Kyushu Institute of Technology*

## 1.1 INTRODUCTION

Parkinson's disease (PD) is a neurogenerative disorder affecting patients' motor and non-motor functions. Due to the lack of dopamine-producing cells in the patient's brain [15,36], their motor abilities start to deteriorate with tremors, slowness of movement (bradykinesia), muscle stiffness (rigidity), and postural instability as PD's cardinal symptoms. Over time, non-motor symptoms manifest, such as mood changes, sleep, speech, and mental difficulties. These motor and non-motor symptoms negatively influence PD patients' daily life and quality of life (QoL) [32].

One of the difficulties experienced by PD patients is called the "wearing-off phenomenon". This phenomenon happens when symptoms reappear earlier than their scheduled Levodopa (L-dopa) treatment intake. L-dopa treatment is one of the best treatments doctors and clinicians prescribe to PD patients to manage their symptoms. Taking an L-dopa dose increases the dopamine production inside the brain, temporarily relieving the patient's symptoms [7]. However, the prolonged use of L-dopa treatment shortens the treatment's effective time. During the wearing-off period, the symptoms re-emerge, causing discomfort to the patients. Thus, PD patients' clinicians must monitor and discuss the wearing-off phenomenon.

DOI: 10.1201/9781003371540-2

Upon assessment by their doctors, they can properly adjust their patients' L-dopa treatment plan or entirely change their treatment [3,8,28,31].

As a contribution to PD management, we forecast future wearing-off in the next hour using the fitness tracker datasets from earlier periods, e.g., data from one day before. Then, existing deep learning architectures were compared to examine the wearing-off forecasting with the fitness tracker features. This chapter's contributions can be summarized by answering these research questions.

1. Can wrist-worn fitness tracker datasets be used to forecast wearing-off in the next hour?

2. Which among the six deep learning architectures performed well in forecasting wearing-off in the next hour?

We used existing and simple deep learning architectures to answer the research questions. Our results showed that a CNN model could forecast the next hour's wearing-off with an average balanced accuracy of 80.64% ± 10.36% across ten participants. Furthermore, the current period's and the previous day's data were necessary for forecasting wearing-off, as both models had high AUC and balanced accuracy scores, respectively. PD patients and clinicians can use the results of this study to monitor and manage PD symptoms during wearing-off periods. PD patients can get early warnings before a wearing-off period. Thus, the PD patient can adapt using such future information. Furthermore, clinicians can deploy personalized forecasting models to collect and monitor wearing-off periods in PD patients.

This chapter is divided into different sections. Section 1.2 provides existing wearing-off prediction models using different datasets from various devices. Section 1.3 describes this chapter's approach to developing wearing-off forecasting models from data collection (Section 1.3.1), data processing (Section 1.3.2), and model development (Section 1.3.3). Then, Sections 24.4 and 1.5 present and discuss the result of the developed forecasting models for wearing-off. Finally, Section 24.5 summarizes the goals of this chapter, along with the future directions of this research.

## 1.2 RELATED STUDIES

This section summarizes existing approaches to detect and predict wearing-off periods among PD patients. In practice, clinicians use their experience and clinical rating scales to regularly assess each patient's PD situation [3,10]. Then, clinicians adjust the PD patients' treatment plan based on their assessment. The latest approaches in monitoring PD patients' symptoms have utilized wearable devices like Parkinson's Kinetigraph (PKG). PKG collects accelerometer data to detect tremors, bradykinesia, and dyskinesia among PD patients. The collected motion data from the PD patients assist clinicians' evaluation of wearing-off [14]. In other studies, various motor-related datasets from accelerometer, gyroscope, and electromyography (EMG) have been used to detect or predict any PD symptoms or wearing-off events. Aside from motor-related datasets, non-motor features from

wearable devices have been introduced to predict wearing-off to understand and match wearing-off periods in terms of non-motor symptoms.

In a literature review conducted on wearable technologies to detect or predict wearing-off, the utilization of wearable devices showed promise in improving the management of PD symptoms. For example, models estimated "on" and "off" states [2] using machine learning algorithms with accelerometer data. In this study, PKG was deployed to collect accelerometer data. Then, different statistical and gait parameters were used to train Random Forest, Support Vector Machine (SVM), k-Nearest Neighbor, and Naive Bayes classifiers to detect "on" and "off" states. Based on its results, the Random Forest classifier produced the best accuracy of 96.72% among the other classifiers, which shows that wearing-off could be detected using accelerometer data [2]. Similarly, other studies have used motion-based datasets, particularly accelerometer data, to detect wearing-off states utilizing different machine learning techniques. Other models have also detected specific PD symptoms. These models produced an accuracy of at least 81% [1,5,16,18,20,26,29]. Given these studies, it was suggested to extend the use of machine learning models to non-motor symptoms in detecting wearing-off [5].

Commercially available fitness trackers' datasets were utilized to predict wearing-off. Two PD participants wore the fitness tracker for 30 days while reporting wearing-off using the Wearing-Off Questionnaire (WoQ-9) [3,11] on their smartphone application [21]. Correlation analysis showed the relationship between PD participants' sleep features and wearing-off symptoms. Intuitively, the time elapsed from the last drug intake strongly predicted wearing-off [35]. Then, each PD participant's prediction model resulted in a balanced accuracy ranging from 70.0% to 76.9% using Gradient Boosting or Logistic Regression learning algorithms. Although the balanced accuracy was lower than those models using motor features from an accelerometer or gyroscope, detecting wearing-off using mainly the non-motor datasets from fitness trackers was feasible [34].

Within the current landscape, detection or prediction models classify whether a PD patient currently suffers wearing-off or not, given the present input features. In the studies mentioned, detection and prediction have been interchangeably used for the classification task. As such, this chapter aims to forecast future wearing-off periods like in the next 30 minutes or 1 hour. Forecasting wearing-off periods drew inspiration from other studies in different domains. Forecasting results provided action points before the event or insights ahead of the anticipated event [23]. For instance, a forecasting model predicted COVID-19 symptoms and signs of viral infection three days before the onset of the symptoms. This study utilized a smart ring's physiological outputs such as heart rate (HR), body temperature, and sleep with the self-reported symptoms from a mobile application [9]. Another similar example used smartwatch data to detect pre-symptomatic COVID-19 cases 4–7 days before the onset of the symptoms [4,22]. In these examples, the insight by the forecasting model provides action points like taking a COVID-19 test. Similarly, this chapter aims to provide similar insights by forecasting future wearing-off events (Table 1.1).

TABLE 1.1 Comparison of Previous Studies on Detecting Specific PD Symptoms or Detecting Eearing-off

| Study | Aim | Data Used | Method | Result |
|---|---|---|---|---|
| Keijsers [20] | Determine between "on" and "off" based on daily activities using wearable data | Accelerometer | Unsupervised method using frequency-based method | Sensitivity: 97%<br>Specificity: 97% |
| Jeon [18] | Classify severity of tremors from wearable data | Accelerometer, gyroscope | Decision Tree (DT), k-Nearest Neighbor (kNN), Random Forest (RF), Support Vector Machine (SVM), Discriminant Analysis | DT: 85.55% accuracy |
| Sama [26] | Detect gait-related disorders using wearable data | Accelerometer | SVM | Accuracy: 91.81% across 12 patients |
| Aich [1] | Detect freezing of gait (FoG) using wearable data | Accelerometer | SVM, kNN, DT, Naive Bayes (NB) | SVM: 88% accuracy |
| Steinmetzer [29] | Detect motor dysfunctions using wearable data | Accelerometer, gyroscope, magnetometer | Convolutional Neural Network (CNN) | Accuracy: 93.40% |

(*Continued*)

TABLE 1.1 (*Continued*) Comparison of Previous Studies on Detecting Specific PD Symptoms or Detecting Eearing-off

| Study | Aim | Data Used | Method | Result |
|---|---|---|---|---|
| Hssayeni [16] | Detect "on" and "off" states | Gyroscope | SVM with fuzzy labeling | Accuracy: 90.5%<br>Sensitivity: 94.2%<br>Specificity: 85.4% |
| Aich [2] | Detect "on" and "off" using gait signals | Accelerometer | RF, SVM, kNN, NB | Accuracy: 96.72%<br>Sensitivity: 97.35% |
| Victorino [34] | Predict "wearing-off" on individual-level | Heart rate, Stress score, Sleep features, Step count | RF, GB, DT, Logistic Regression (LR), Linear SVM | Balanced accuracy<br>Participant 1: 70.00%–71.70%<br>Participant 2: 76.10%–76.90% |
| Current study | Forecasting next hour "wearing-off" on individual-level | Heart rate, stress score, sleep features, step count | Multilayer perceptron (MLP), Long short-term memory (LSTM), CNN | Balanced accuracy<br>$80.64\% \pm 10.36\%$<br>across ten patients |

## 1.3 METHODOLOGY

This section describes (1) how the datasets were collected from the PD patients, (2) how the data was processed for model development, and (3) how each deep learning architecture was developed to forecast wearing-off. This chapter introduces the feasibility of forecasting wearing-off from fitness tracker datasets in previous periods. As such, the target wearing-off forecast is 1-hour into the future. The following subsections detail the data collection, processing, and model development.

### 1.3.1 Data Collection

The data collection process was similar to the previous work on understanding and predicting wearing-off among the two PD patients [34,35]. The Garmin vivosmart4 fitness trackers were distributed to PD participants to collect the heart rate, stress score, sleep data, and step count. In addition, Android smartphones were provided to the PD participants with the needed applications. These two tools mainly collected fitness tracker datasets and wearing-off periods among PD participants.

Both tools collect and send data from PD participants to their respective servers. On the one hand, vivosmart4 sends data to the Garmin Connect smartphone application through Bluetooth. Then, Garmin Connect uploads the received data to Garmin servers. Finally, collected datasets were accessed using Garmin Health API.[1] On the other hand, PD patients answered different questionnaires through a customized smartphone application. The wearing-off questionnaire asked what symptoms were experienced, and when the symptoms started and ended. The data collected from PD participants were received by different servers, as illustrated in Figure 1.1 [34,35].

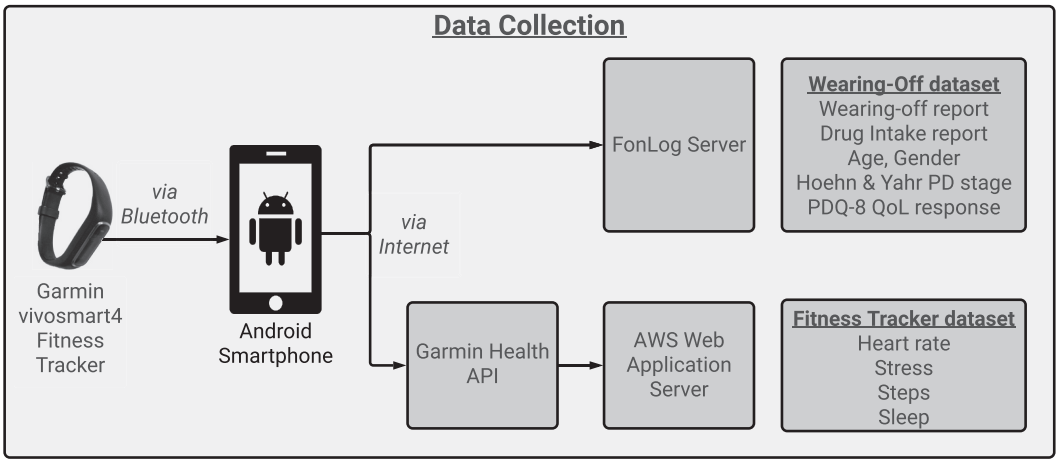


Figure 1.1 The data collection process from the tools to the servers where each dataset can be accessed [34].

TABLE 1.2 Garmin Vivosmart4 Collected Datasets via Garmin Health API

| Dataset | Interval | Description |
|---|---|---|
| Heart rate | 15-second | Beats per minute |
| steps | 15-minute | Cumulative step count per interval, with 0 as the lowest value |
| Stress score | 3-minute | Estimated stress score [13]<br>• 0–25: resting state,<br>• 26–50: low stress,<br>• 51–75: medium stress,<br>• 76–100: high stress,<br>• −1: not enough data to detect stress,<br>• −2: too much motion |
| Sleep stages with each sleep duration | Varying interval for each date | Start and end time for each sleep stage [12]<br>• Light sleep<br>• Rapid eye movement (REM) sleep<br>• Deep sleep<br>• Awake |

Various datasets collected and provided by each tool were also presented in Figure 1.1. For the vivosmart4 fitness tracker, Garmin Health API provides access to the heart rate, stress score, number of steps, and sleep duration for each sleep stage. Each dataset from Garmin Health API comes in different time intervals. The heart rate (HR) in beats per minute (bpm) is reported every 15 seconds. Meanwhile, the number of steps is accumulated every 15 minutes. Then, the stress score is estimated by Garmin's algorithm. Stress scores are estimated every 3 minutes, ranging from 0 to 100, where 100 is the most stressful. Stress scores can also be reported with "-1" and "-2" for insufficient data and too much motion, respectively [24,30]. Finally, the sleep duration is grouped by date and by sleep stages [12] (Table 1.2).

For the smartphone application, the wearing-off periods, drug intake time and its effect on each wearing-off symptom, and other basic information were collected from PD participants. PD participants manually answered each questionnaire. The wearing-off periods, the drug intake time, and the drug effects were recorded using the Japanese version of the Wearing-Off Questionnaire (WoQ-9). The first part of the WoQ-9 asked PD participants whether they experienced these nine wearing-off symptoms or not [3,11]. In addition, the PD participants had to specify when the symptoms started and ended.

1. Tremors,
2. Slowing down of movement,
3. Change in mood or depression,
4. Rigidity of muscles,

5. Sharp pain or prolonged dull pain,
6. Impairment of complex movements of the hand & fingers,
7. Difficulty integrating thoughts or slowing down of thoughts,
8. Anxiety or panic attacks, and
9. Muscle spasm.

Then, the second part of the WoQ-9 asked about the drug intake time and its effects. The PD participant had to indicate whether each symptom subsided or not. Other pieces of information were asked using the smartphone application, such as age, sex, Hoehn and Yahr (H&Y) scale, the Japan Ministry of Health, Labor, and Welfare's classification of living dysfunction (JCLD) for the PD stage [6,19], and the Parkinson's Disease Questionnaire (PDQ-8) for the PD patient's self-assessed quality of life [17]. These datasets are summarized in Table 1.3.

This research study has received the University's ethical review. Meanwhile, the two tools were distributed to PD participants. PD participants can participate in this research if (1) they experience wearing-off, (2) they can use the tools, and (3) they do not have any severe illnesses or symptoms that could affect them during the data collection period. PD participants are referred to either by their doctor or by other PD patients. Before starting the data collection period, PD patients were informed of the research goals. Then, we asked for their written consent. Afterward, the tools were distributed to begin the data collection period. PD participants were asked to contribute seven (7) days' worth of data. However, they can freely discontinue or opt out of the research study if they cannot proceed with the data collection.

During the data collection period, participants were asked to wear the Garmin vivosmart4 every time, even when taking a bath or sleeping. Meanwhile, it is important to wear it during the night to capture the sleep duration data. On the other hand, recording the participant's wearing-off at their own convenient time

TABLE 1.3 The Smartphone Application Collected Datasets

| Data Type | Description |
|---|---|
| WoQ-9 | Symptoms onset and drug intake time |
| Basic Information | Age and gender |
| Hoehn and Yahr Scale (H&Y), Japan Ministry of Health, Labor, and Welfare's classification of living dysfunction (JCLD) | Participant's PD stage |
| PDQ-8 | Participant's QoL measurement specific to PD: 0%–100%, with 100% showing the worst QoL |

was emphasized to the participants. Using the smartphone application was suggested during their "on" state or when their wearing-off symptoms are less severe. In addition, PD participants were instructed to correct and review their responses with the correct time in the application. Aside from the previously stated constraints and suggestions, there were no strict limitations during the data collection period.

### 1.3.2 Data Processing

The Garmin vivosmart4 and smartphone application wearing-off datasets were processed and combined to develop the wearing-off forecasting model. This section describes the data processing for each dataset and the combined dataset.

On the one hand, the raw Garmin vivosmart4 datasets were cleaned, processed, and re-sampled to the chosen time interval. First, missing values were supplied with "−1," like how Garmin supplied missing values [12]. A value of "−1" also indicated that the fitness tracker was not worn. Next, each fitness tracker dataset was re-sampled due to different intervals provided by Garmin Health API, as shown in Table 1.2. The combined dataset was re-sampled into 15-minute intervals to match the highest interval provided by Garmin. The last available data was used to fill the missing values caused by the re-sampling. Finally, the sleep duration for each sleep phase was distributed in each record by its calendar date. Additional sleep features were extracted from the sleep dataset as shown in Equations 1.1– 1.4 [25,27].

$$\text{Total non-REM duration} = \text{Deep sleep duration} + \text{Light sleep duration}, \tag{1.1}$$

$$\text{Total sleep duration} = \text{Total non-REM duration} + \text{REM sleep duration} \tag{1.2}$$

$$\text{Total non-REM percentage} = \frac{\text{Total non-REM duration}}{\text{Total sleep duration}} \tag{1.3}$$

$$\text{Sleep efficiency} = \frac{\text{Total sleep duration}}{\text{Total sleep duration} + \text{Total awake duration}} \tag{1.4}$$

On the other hand, the raw smartphone application dataset was also transformed like with raw Garmin vivosmart4 datasets. First, overlapping wearing-off periods were combined into one wearing-off period. Then, each wearing-off report was matched with the re-sampled 15-minute timestamp. If wearing-off falls within the interval, a value of "1" was assigned for the wearing-off symptom. Otherwise, the wearing-off symptom was given a value of "0". Likewise, the drug intake reports and their effect on the symptom were processed to match each timestamp. If the symptom subsided after taking medicine, the symptom was marked with "0". However, if the symptom was still experienced, the value of "1" was kept.

Finally, the two datasets were combined by matching the 15-minute timestamp. The hour of the day and the day of the week were also included. The day of the week was encoded with "0" to "6", matching "Monday" to "Sunday." Meanwhile, the hour of the day was encoded using sine and cosine functions. Finally, the following features were used to develop the wearing-off forecasting model.

$x_1$: Heart rate (HR)

$x_2$: Step count (Steps)

$x_3$: Stress score (Stress)

$x_4$: Awake duration during the estimated sleep period (Awake)

$x_5$: Deep sleep duration (Deep)

$x_6$: Light sleep duration (Light)

$x_7$: REM sleep duration (REM)

$x_8$: Total non-REM sleep duration (NonREMTotal)

$x_9$: Total sleep duration (Total)

$x_{10}$: Total non-REM sleep percentage (NonREMPercentage)

$x_{11}$: Sleep efficiency (SleepEfficiency)

$x_{12}$: Day of the week (TimestampDayOfWeek)

$x_{13}$: Sine value of Hour of the day (TimestampHourSin)

$x_{14}$: Cosine value of Hour of the day (TimestampHourCos)

$y$: Wearing-off

### 1.3.3 Model Development

This section presents the development of the wearing-off forecasting model. This section includes the data split specification among training, validation, and test sets, the metrics used to evaluate the forecasting model, and the architectures considered in developing the wearing-off forecasting model. The wearing-off forecast models were built individually per PD participant because it was assumed that each PD participant experienced PD differently. The data processing and model development used different Python libraries such as Pandas, Tensorflow, and Keras.

The wearing-off forecasting models were built for each PD participant. Individualized forecasting models were built instead of a general forecasting model because this chapter assumes that each patient experiences PD differently. Then, each PD participant's dataset was divided sequentially into training, validation, and test sets. The first 60% of the PD participant's dataset was used for training, while the next 20% was used for validation. The final 20% of the PD patient's dataset was held out to test and evaluate the forecasting model on different metrics. The balanced accuracy (*Bal.Acc.*) was the main metrics to evaluate the developed wearing-off forecast models because of the imbalance in the dataset. *Bal.Acc.* took into consideration the distribution of wearing-off within the PD participants' datasets, as shown in

Equation 1.5. Other than *Bal.Acc.*, *Accuracy*, *F*1*Score*, *Precision*, *Recall*, and *AUC* were also reported and calculated as follows:

$$\text{Bal. Acc.} = \frac{\frac{\text{TP}}{P} + \frac{\text{TN}}{N}}{2}, \tag{1.5}$$

$$\text{Accuracy} = \frac{\text{TP} + \text{TN}}{\text{TP} + \text{FP} + \text{TN} + \text{FN}}, \tag{1.6}$$

$$\text{F1 Score} = \frac{2 \cdot \text{TP}}{2 \cdot \text{TP} + \text{FP} + \text{FN}}, \tag{1.7}$$

$$\text{Precision} = \frac{\text{TP}}{\text{TP} + \text{FP}}, \tag{1.8}$$

$$\text{Recall} = \frac{\text{TP}}{\text{TP} + \text{FN}}, \tag{1.9}$$

TP is the number of true positives where the predicted wearing-off is equal to the actual wearing-off ("1"), while TN is the number of true negatives where the predicted normal state is equal to the actual normal state ("0"). Then, $P$ is the total number of wearing-offs, and $N$ is the total number of a normal state. Finally, FP is the number of false positives or where the predicted value is wearing-off, but the actual value is a normal state, and FN is the number of false negatives or where the predicted value is a normal state, but the actual value is wearing-off.

#### 1.3.3.1 Experiments

In terms of deep learning architectures, there were six architectures considered in this chapter. Equation 1.10 defines the general model of the six architectures.

$$y_{t+1} = f(X_t, y_t), X_t = \{x_1, x_2, \ldots, x_{14}\} \tag{1.10}$$

In finding the wearing-off in the next hour $y_{t+1}$, the models accept the 14 features $X_t = \{x_1, x_2, \ldots, x_{14}\}$ at the current time $t$ explained in Section 1.3.2. The models also accept the wearing-off at the current time $y_t$. Equation 1.10 summarizes the first three architectures, *Baseline*, *Linear*, and *Single time-step Dense*.

The *Baseline* architecture copied the wearing-off label into the next hour $t_1$. Next, the *Linear* architecture or a multi-layer perceptron model applied a linear transformation in the form of a single *Dense* layer. Another version of the *Linear* architecture contained more *Dense* layers to compare how adding more layers differed from a single *Dense* layer. As specified in Equation 1.10, these first three architectures only used the features at the current time to forecast the next hour. Hence, no historical context has been incorporated into these architectures [33].

The following three architectures used multiple time steps to forecast wearing-off in the next hour. Equation 1.11 accepts a matrix $M$ of 14 features and wearing-off

in previous time steps from the current time until $w$ time step before the current time. This chapter used the last day's data ($w = 23$).

$$y_{t+1} = f(M(X, y, w)), M = \begin{bmatrix} X_t & y_t \\ X_{t-1} & y_{t-1} \\ \vdots & \vdots \\ X_{t-w} & y_{t-w} \end{bmatrix} \tag{1.11}$$

The *Multi time-step Dense* architecture extended the *Single time-step Dense* architecture by accepting 1-day's worth of input data $t_0 \dots t_{24}$. Each time step was flattened as another set of features before passing onto the two *Dense* layers. Like the *Multi time-step Dense* architecture, the *CNN* architecture incorporated multiple time steps as its input. However, the *CNN* architecture step had an initial *Conv*1*D* layer that could accept an input of any length. On the other hand, the *Multi time-step Dense* architecture could only accept a fixed input length. Finally, the *LSTM* architecture has been considered well-suited for time-series data since it keeps an internal state from one time step to the subsequent step [33]. Table 1.4 provides the specification of each architecture.

Finally, the models were implemented in a computer with an Intel i7-6700 CPU @ 3.40 GHz with four cores and 16 GB RAM. The architectures were trained with the following set of hyperparameters. The maximum number of epochs was fixed at 200, with an early stopping mechanism based on the validation's loss until ten epochs. A binary cross-entropy loss function was used for training the models. Then, the Adam algorithm was used for optimization with a learning rate of 0.001. Eight mini-batches were also produced for training each model.

TABLE 1.4 Architectures Considered for Wearing-off Forecast Model [33]

| **Architecture** | **Input** | **Output** | **Layers** |
|---|---|---|---|
| Baseline | $t_0$ | $t_1$ | N/A |
| Linear | $t_0$ | $t_1$ | Dense(1, sigmoid) |
| Single time-step dense | $t_0$ | $t_1$ | Dense(64, ReLu) |
| | | | Dense(64, ReLu) |
| | | | Dense(1, sigmoid) |
| Multi time-step dense | $t_0 \dots t_{23}$ | $t_{24}$ | Flatten |
| | | | Dense(64, ReLu) |
| | | | Dense(64, ReLu) |
| | | | Dense(1, sigmoid) |
| CNN | $t_0 \dots t_{23}$ | $t_{24}$ | Conv1D((64, 24), ReLu) |
| | | | Dense(64, ReLu), |
| | | | Dense(1, sigmoid) |
| LSTM | $t_0 \dots t_{23}$ | $t_{24}$ | LSTM(16, return_sequence=True) |
| | | | Dense(1, sigmoid) |

Each architecture forecasts the wearing-off in the next hour ($t_1$ or $t_{24}$), given previous fitness tracker features and wearing-off ($t_0$ or $t_0 \dots t_{23}$).

## 1.4 RESULTS

In this chapter, we have built wearing-off forecasting models for each of the 10 PD participants who joined the research study. The 7-day data collection started upon their written consent. Some PD participants have contributed more than others. In contrast, two participants lacked the number of days needed due to the discomfort caused by their symptoms or for other reasons. This variation in the data collection duration resulted in an average of 9 days ± 1.826. In general, PD participants have met the prescribed 7-day data collection since the average PD stage of the participants was 2.8 ± 0.632 on Hoehn & Yahr Scale, while 1.7 ± 0.483 for Japan's Ministry of Health, Labor, and Welfare's Classification of Impairment of Life Function. The average PD stage was characterized by shaking of either or both limbs, muscle stiffness on either or both sides, no to mild physical disability, and some inconvenience with daily life [6,19]. Furthermore, PD participants' self-reported quality of life according to their PDQ-8 response was 42.50% ± 0.192, which indicated a low to middle quality of life for a PD patient (Table 1.5).

### 1.4.1 Can Wrist-worn Fitness Tracker Datasets Be Used to Forecast Wearing-off in the Next Hour?

Each PD participant's model was able to forecast 1-hour future wearing-off. With the current time's fitness tracker datasets and the current wearing-off status. The single time-step dense forecasting model provided the highest *Bal.Acc.* and *AUC* scores of 79.05% ± 7.09% and 69.14% ± 10.60%. Meanwhile, with 1-day's worth of fitness tracker datasets and wearing-off periods, the CNN model showed the highest *Bal.Acc.* and *AUC* scores of 80.64% *pm* 10.36% and 60.52% *pm* 30.26%, respectively. These results showed that we could forecast wearing-off in the next hour, either with the current period or with the previous day's fitness tracker datasets and wearing-off periods.

TABLE 1.5 The Participants Demographics

| Participant | Age | Gender | H&Y | JCLD | PDQ-8 | Number of Collection Days |
|---|---|---|---|---|---|---|
| **1** | 43 | Female | 2 | 1 | 37.50% | 9 |
| **2** | 38 | Female | 3 | 2 | 65.63% | 6 |
| **3** | 49 | Female | 3 | 2 | 34.38% | 10 |
| **4** | 69 | Female | 3 | 1 | 78.13% | 10 |
| **5** | 49 | Female | 2 | 2 | 37.50% | 8 |
| **6** | 56 | Female | 2 | 2 | 37.50% | 9 |
| **7** | 48 | Male | 3 | 1 | 15.63% | 6 |
| **8** | 77 | Male | 3 | 2 | 34.38% | 11 |
| **9** | 84 | Male | 4 | 2 | 59.38% | 11 |
| **10** | 58 | Male | 3 | 2 | 25.00% | 10 |
| **Average** | 57.1 | | 2.8 | 1.7 | 42.50% | 9 |
| **Std. Dev.** | 15.059 | | 0.632 | 0.483 | 0.192 | 1.826 |

TABLE 1.6 Wearing-Off Forecast Model Performance

| **Architectures** | **Bal. Acc. (%)** | **AUC (%)** | **Accuracy (%)** |
|---|---|---|---|
| Baseline | 79.05 ± 7.09 | 50.20 ± 5.68 | 86.97 ± 7.19 |
| Linear | 79.05 ± 7.09 | 64.71 ± 16.25 | 70.33 ± 28.13 |
| Single time-step dense | 79.05 ± 7.09 | 69.14 ± 10.60 | 92.49 ± 3.62 |
| Multi time-step dense | 80.64 ± 10.36 | 60.23 ± 28.33 | 81.73 ± 26.99 |
| CNN | 80.64 ± 10.36 | 60.52 ± 30.26 | 85.09 ± 12.41 |
| LSTM | 50.00 ± 0.00 | 57.83 ± 17.13 | 85.67 ± 10.73 |
| **Architectures** | **Precision (%)** | **Recall (%)** | **F1 Score (%)** |
| Baseline | 7.81 ± 10.16 | 7.59 ± 9.66 | 7.69 ± 9.90 |
| Linear | 5.08 ± 6.34 | 28.73 ± 33.58 | 8.09 ± 9.68 |
| Single time-step dense | 6.25 ± 13.50 | 6.15 ± 15.83 | 5.10 ± 11.37 |
| Multi time-step dense | 18.55 ± 32.29 | 36.17 ± 42.24 | 20.40 ± 29.72 |
| CNN | 18.61 ± 31.98 | 25.06 ± 39.10 | 15.58 ± 21.31 |
| LSTM | 3.20 ± 5.17 | 8.10 ± 14.78 | 3.83 ± 6.24 |

The reported metric scores were averaged across the individual metric scores for each participant. While some participants had extremely low precision, recall, and F1 scores.

### 1.4.2 Which among the Six Deep Learning Architectures Performed Well in Forecasting Wearing-off in the Next Hour?

Among the six architectures considered in this chapter, single time-step Dense, multi time-step dense, and CNN models produced the best metric scores. Both multi time-step Dense model and the CNN model had the best *Bal.Acc.* across all 10 PD participants. However, the CNN model produced the highest precision and recall scores of 18.61% ± 31.98% and 36.17% ± 42.24%. Our results have shown that despite being used prominently in time-series datasets, the LSTM model performed the worst among the architectures and just a little above the Baseline model. However, this chapter did not optimize the hyperparameters or customize each architecture. Table 1.6 presents how each architecture performed in each metric.

## 1.5 DISCUSSIONS

The multi time-step dense and CNN models produced similar results across all metrics. These two architectures were the same, except that the CNN model can accept varying input lengths. The CNN model's first layer handled the sliding window to accommodate the variation in input data. Despite having a similar architecture, the multi time-step dense model provided the highest recall score among all architectures. However, the recall score was lower than 50%. We wanted a higher recall score because we did not want the forecasting model to miss a wearing-off event. For example, the wearing-off forecasting model was deployed to notify the PD participant whether a wearing-off could happen in the next hour. With the current highest recall score, the forecasting model missed informing the actual wearing-off events. These missed events were illustrated in the confusion matrix (Figure 1.2),

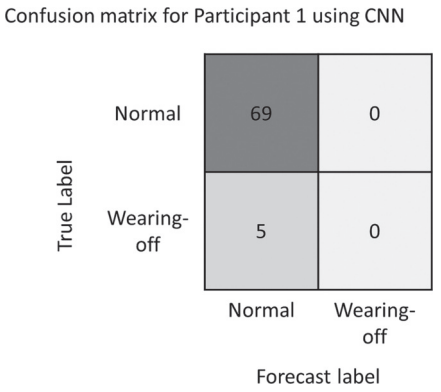


Figure 1.2 Confusion matrix produced by the CNN model using participant 1's combined data. The CNN model for participant 1 failed to forecast the wearing-off label (TP = 0). A similar confusion matrix with TP = 0 was evident among the other five participants.

where the forecasting model had missed all the actual wearing-off events. Five participants had zero recall scores with multi time-step dense model. In comparison, six participants had zero recall with the CNN model. These cases caused the average recall, precision, and F1 scores to have low scores.

Within the context of a notification application for PD patients, we wanted a higher recall score because we did not want to miss actual wearing-off. However, we also wanted to minimize false positives because we did not want to overwhelm the PD patients with the notifications, only to end up as false alarms. The AUC metric balances the true positive rate or recall and the false positive rate. That was why the single time-step dense model had also been considered due to having the highest AUC score.

Finally, Figures 1.3 and 1.4 present the sample forecast made by the model. For participant 10's sample forecast (Figure 1.3), the forecast at $t_{25}$ and $t_{26}$ matched the ground truth labels. However, for participant 6's sample forecast (Figure 1.4), the forecast at $t_{25}$ did not exceed the 0.5 default threshold, despite having increased forecast probability. These results and observations happened with other participants' forecasts, affecting the metric scores. Thus, optimizing the threshold value for each PD patient's forecasting model should be considered in future work.

## 1.6 CONCLUSION

This chapter demonstrates that deep learning models can forecast wearing-off in the next hour using wrist-worn fitness tracker datasets. The PD patients used the wrist-worn fitness tracker for nine days on average to collect their heart rate, stress score, sleep duration in each sleep stage, and the number of steps. The trained deep learning models have forecasted wearing-off in the next hour, given either the current time or the previous day's dataset as input to the model. The deep learning

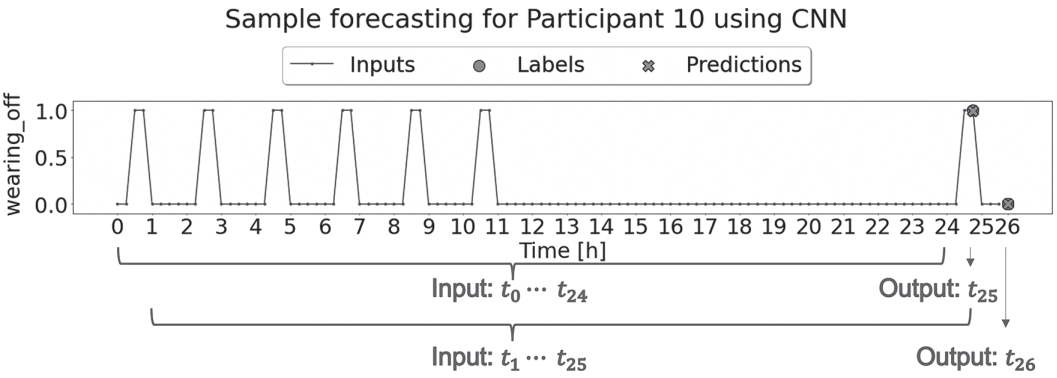


Figure 1.3 Sample wearing-off forecasting using the CNN model with participant 10's combined data. The CNN model used the last day's data (Input: $t_0 \ldots t_{24}$) to forecast the next hour's wearing off (Output: $t_{25}$). The forecast was marked with "X" while the ground truth was labeled with "O". The y-axis represented the forecast probabilities with "0" as no wearing-off and "1" as wearing-off.

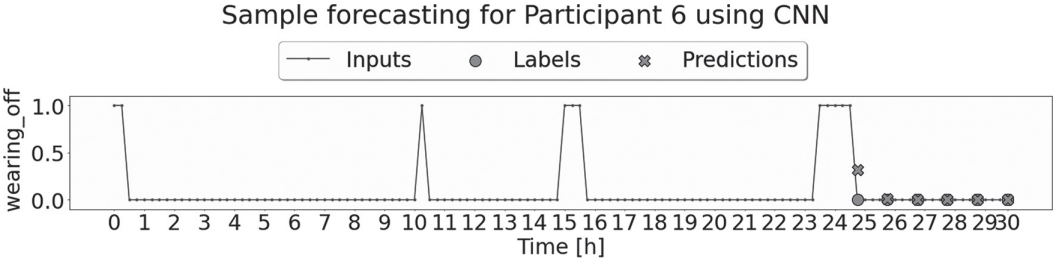


Figure 1.4 Sample wearing-off forecasting using the CNN model with participant 6's combined data. At the time $t_{25}$, the forecast had a slightly higher forecast probability but was not considered with a wearing-off label of 1.

models have performed well compared to the baseline model, which only copied the last period's wearing-off state. However, the models can still be improved to minimize false positives and negatives in their forecast.

As shown in the sample wearing-off forecasts, the best architecture in this paper (CNN model) showed increased probability scores during actual wearing-off periods. However, it was lower than the default 50% threshold for wearing-off. The threshold level can be optimized for each PD participant's model in future work to reduce the false negative and provide a better future forecast. These can be achieved by fine-tuning the architecture's hyperparameters, modifying the loss function, or giving hidden states that consider prior information about wearing-off.

This chapter has shown that the wearing-off forecasting model can use either the previous day's data or only the current period's data. The Single time-step Dense model used only the current period's data and produced the highest AUC score. Meanwhile, the CNN model had the highest *Bal.Acc.* given the previous

day's data. These results lead to future work balancing the historical context of the wearing-off and the current wearing-off state. The historical data taught the forecasting model patterns on when wearing-off could occur, e.g., what hour of the day or at which heart rate or stress score wearing-off occurs. Meanwhile, the current wearing-off provides immediate state of the patient, like when a wearing-off period has begun, and PD patient has shown an extended period of wearing-off. Thus, future forecasting models should be able to balance the historical and the current information while identifying the best-suited forecasting period 15, 30 minutes, or 1 hour into the future.

Finally, in real-life applications, wearing-off reports were not immediately accessible. For example, this scenario happens when forecasting models are trained to accept the current wearing-off state. PD patients report wearing-off after the event occurs; as such, the current wearing-off state is unknown. The forecasting model should provide probability distribution for the missing current wearing-off in future work. Then, the model will use that current period's probability distribution to forecast wearing-off in the next hour. The model should dynamically update the probabilities given the new information when the PD patient reports the actual wearing-off periods. This last suggestion will benefit PD patients in real-life applications where patients and their clinicians can be asked to label only specific periods. The targetted labeling should produce the optimal changes in the forecasting model. This system allows monitoring and reporting of wearing-off and PD patients' symptoms while the models yield actionable insights.

## Note

1. https://developer.garmin.com/gc-developer-program/health-api/

## BIBLIOGRAPHY

[1] Satyabrata Aich, Pyari Mohan Pradhan, Jinse Park, Nitin Sethi, Vemula Sai Sri Vathsa, and Hee-Cheol Kim. A validation study of freezing of gait (FoG) detection and machine-learning-based FoG prediction using estimated gait characteristics with a wearable accelerometer. *Sensors*, 18(10):3287, 2018.

[2] Satyabrata Aich, Jinyoung Youn, Sabyasachi Chakraborty, Pyari Mohan Pradhan, Jinhan Park, Seongho Park, and Jinse Park. A supervised machine learning approach to detect the on/off state in Parkinson's disease using wearable based gait signals. *Diagnostics*, 10(6):421, 2020.

[3] Angelo Antonini, Pablo Martinez-Martin, Ray K. Chaudhuri, Marcelo Merello, Robert Hauser, Regina Katzenschlager, Per Odin, Mark Stacy, Fabrizio Stocchi, Werner Poewe, Oliver Rascol, Cristina Sampaio, Anette Schrag, Glenn T. Stebbins, and Christopher G. Goetz. Wearing-off scales in Parkinson's disease: Critique and recommendations: Scales to assess wearing-off in PD. *Movement Disorders*, 26(12):2169–2175, 2011.

[4] H. Ceren Ates, Ali K. Yetisen, Firat Güder, and Can Dincer. Wearable devices for the detection of COVID-19. *Nature Electronics*, 4(1):13–14, 2021.

[5] Mercedes Barrachina-Fernández, Ana María Maitín, Carmen Sánchez-Ávila, and Juan Pablo Romero. Wearable technology to detect motor fluctuations in Parkinson's disease patients: Current state and challenges. *Sensors*, 21(12):4188, 2021.

[6] Roongroj Bhidayasiri and Daniel Tarsy. Parkinson's disease: Hoehn and Yahr Scale. In Roongroj Bhidayasiri and Daniel Tarsy, editors, *Movement Disorders: A Video Atlas (Current Clinical Neurology)*, pp. 4–5. Humana Press: Totowa, NJ, 2012.

[7] Cleveland Clinic. Parkinson's disease: Causes, symptoms, stages, treatment, support, 2022.

[8] Delia Colombo, Giovanni Abbruzzese, Angelo Antonini, Paolo Barone, Gilberto Bellia, Flavia Franconi, Lucia Simoni, Mahmood Attar, Emanuela Zagni, Shalom Haggiag, and Fabrizio Stocchi. The "gender factor" in wearing-off among patients with Parkinson's disease: A Post Hoc Analysis of DEEP study, 2015.

[9] Pierre-François D'Haese, Victor Finomore, Dmitry Lesnik, Laura Kornhauser, Tobias Schaefer, Peter E. Konrad, Sally Hodder, Clay Marsh, and Ali R. Rezai. Prediction of viral symptoms using wearable technology and artificial intelligence: A pilot study in healthcare workers. *PLoS One*, 16(10):e0257997, 2021.

[10] Parisa Farzanehfar, Holly Woodrow, and Malcolm Horne. Assessment of wearing off in Parkinson's disease using objective measurement. *Journal of Neurology*, 268(3):914–922, 2021.

[11] Jiro Fukae, Masa-aki Higuchi, Shosaburo Yanamoto, Kosuke Fukuhara, Jun Tsugawa, Shinji Ouma, Taku Hatano, Asako Yoritaka, Yasuyuki Okuma, Kenichi Kashihara, Nobutaka Hattori, and Yoshio Tsuboi. Utility of the Japanese version of the 9-item wearing-off questionnaire. *Clinical Neurology and Neurosurgery*, 134:110–115, 2015.

[12] Garmin. Garmin vivosmart 4, 2020.

[13] Garmin. Vívosmart 4 - heart rate variability and stress level, 2020.

[14] Robert I. Griffiths, Katya Kotschet, Sian Arfon, Zheng Ming Xu, William Johnson, John Drago, Andrew Evans, Peter Kempster, Sanjay Raghav, and Malcolm K. Horne. Automated assessment of Bradykinesia and Dyskinesia in Parkinson's disease. *Journal of Parkinson's Disease*, 2(1):47–55, 2012.

[15] Sietske Heyn and Charles Patrick Davis. Parkinson's disease early and later symptoms, 5 stages, and prognosis, 2020.

[16] Murtadha D. Hssayeni, Michelle A. Burack, Joohi Jimenez-Shahed, and Behnaz Ghoraani. Assessment of response to medication in individuals with Parkinson's disease. *Medical Engineering & Physics*, 67:33–43, 2019.

[17] Crispin Jenkinson, Ray Fitzpatrick, Viv Peto, Richard Greenhall, and Nigel Hyman. The PDQ-8: Development and validation of a short-form Parkinson's disease questionnaire. *Psychology & Health*, 12(6):805–814, 1997.

[18] Hyoseon Jeon, Woongwoo Lee, Hyeyoung Park, Hong Ji Lee, Sang Kyong Kim, Han Byul Kim, Beomseok Jeon, and Kwang Suk Park. Automatic classification of tremor severity in Parkinson's disease using a wearable device. *Sensors*, 17(9):2067, 2017.

[19] K. Kashiwara, A. Takeda, and T. Maeda. みんなで学ぶパーキンソン病：患者さんとともに歩む診療をめざして QA付き *(Learning Parkinson's disease together with patients: Toward a medical practice that works with patients, with Q&A)*. Nankodo, Tokyo, Japan, 2013.

[20] Noël L. W. Keijsers, Martin W. I. M. Horstink, and Stan C. A. M. Gielen. Ambulatory motor assessment in Parkinson's disease. *Movement Disorders*, 21(1):34–44, 2006.

[21] Nattaya Mairittha, Tittaya Mairittha, and Sozo Inoue. A mobile app for nursing activity recognition. In *Proceedings of the 2018 ACM International Joint Conference and 2018 International Symposium on Pervasive and Ubiquitous Computing and Wearable Computers*, Singapore, pp. 400–403, 2018.

[22] Tejaswini Mishra, Meng Wang, Ahmed A. Metwally, Gireesh K. Bogu, Andrew W. Brooks, Amir Bahmani, Arash Alavi, Alessandra Celli, Emily Higgs, Orit Dagan-Rosenfeld, Bethany Fay, Susan Kirkpatrick, Ryan Kellogg, Michelle Gibson, Tao Wang, Erika M. Hunting, Petra Mamic, Ariel B. Ganz, Benjamin Rolnik, Xiao Li, and Michael P. Snyder. Pre-symptomatic detection of COVID-19 from smartwatch data. *Nature Biomedical Engineering*, 4(12):1208–1220, 2020.

[23] Senthilkumar Mohan, A. John, Ahed Abugabah, M. Adimoolam, Shubham Kumar Singh, Ali Kashif Bashir, and Louis Sanzogni. An approach to forecast impact of Covid-19 using supervised machine learning model. *Software: Practice and Experience*, 52(4):824–840, 2022.

[24] Nanna J. Mouritzen, Lisbeth H. Larsen, Maja H. Lauritzen, and Troels W. Kjær. Assessing the performance of a commercial multisensory sleep tracker. *PLoS One*, 15(12):e0243214, 2020.

[25] David L. Reed and William P. Sacco. Measuring sleep efficiency: What should the denominator be? *Journal of Clinical Sleep Medicine : JCSM : Official Publication of the American Academy of Sleep Medicine*, 12(2):263–266, 2016.

[26] A. Samà, C. Pérez-López, D. Rodríguez-Martín, A. Català, J. M. Moreno-Aróstegui, J. Cabestany, E. de Mingo, and A. Rodríguez-Molinero. Estimating bradykinesia severity in Parkinson's disease by analysing gait through a waist-worn sensor. *Computers in Biology and Medicine*, 84:114–123, 2017.

[27] Lynn A. Schroeder, Olivier Rufra, Nicolas Sauvageot, François Fays, Vannina Pieri, and Nico J. Diederich. Reduced rapid eye movement density in Parkinson disease: A polysomnography-based case-control study. *Sleep*, 39(12):2133–2139, 2016.

[28] Mark Stacy, Robert Hauser, Wolfgang Oertel, Anthony Schapira, Kapil Sethi, Fabrizio Stocchi, and Eduardo Tolosa. End-of-dose wearing off in Parkinson disease: A 9-question survey assessment. *Clinical Neuropharmacology*, 29(6):312–321, 2006.

[29] Tobias Steinmetzer, Michele Maasch, Ingrid Bonninger, and Carlos M. Travieso. Analysis and classification of motor dysfunctions in arm swing in Parkinson's disease. *Electronics*, 8(12):1471, 2019.

[30] Suzanne Stevens and Catherine Siengsukon. Commercially-available wearable provides valid estimate of sleep stages. *Neurology*, 92(15 Supplement): P3.6-042, 2019.

[31] F. Stocchi, A. Antonini, P. Barone, M. Tinazzi, M. Zappia, M. Onofrj, S. Ruggieri, L. Morgante, U. Bonuccelli, L. Lopiano, P. Pramstaller, A. Albanese, M. Attar, V. Posocco, D. Colombo, and G. Abbruzzese. Early detection of wearing off in Parkinson disease: The deep study. *Parkinsonism & Related Disorders*, 20(2):204–211, 2014.

[32] Sigurlaug Sveinbjornsdottir. The clinical symptoms of Parkinson's disease. *Journal of Neurochemistry*, 139(S1):318–324, 2016.

[33] Tensorflow. Time series forecasting. https://www.tensorflow.org/tutorials/structured_data/time_series, June 2022.

[34] John Noel Victorino, Yuko Shibata, Sozo Inoue, and Tomohiro Shibata. Predicting wearing-off of Parkinson's disease patients using a wrist-worn fitness tracker and a smartphone: A case study. *Applied Sciences*, 11(16):7354, 2021.

[35] John Noel Victorino, Yuko Shibata, Sozo Inoue, and Tomohiro Shibata. Understanding wearing-off symptoms in Parkinson's disease patients using wrist-worn fitness tracker and a smartphone. *Procedia Computer Science*, 196:684–691, 2022.

[36] K. Yamabe, H. Kuwabara, R. Liebert, and I. Umareddy. The burden of Parkinson's disease(Pd) in Japan. *Value in Health*, 19(7):A435, 2016.

# Toward Human Thermal Comfort Sensing: New Dataset and Analysis of Heart Rate Variability (HRV) Under Different Activities

**Tahera Hossain, Yusuke Kawasaki, Kazuki Honda, Kizito Nkurikiyeyezu, and Guillaume Lopez**

*Aoyama Gakuin University*

## 2.1 INTRODUCTION

Thermal comfort is a mental state characterized by satisfaction with one's thermal environment, which is critical for everyday productivity [5,25], safety [33], and human well-being [24,34]. Existing research [6,30] indicates that thermal discomfort has an impact on occupiers' productivity as well as their long-term health. Long-term exposure to high temperatures can result in cardiac issues or heart failure (heat stroke), whereas prolonged exposure to cold temperatures lowers the core temperature, which can cause drowsiness, lethargy, and even death. On a broad scale, the relationship between heat stress, health, and performance is well recognized. However, the physiological elements that affect a worker's vulnerability are still up for debate. Therefore, increasing a person's or a group's level of comfort is a worthwhile goal.

As specified in thermal comfort standards such as ASHRAE Standard 55 [2,7], EN 15251 [1], and ISO 7730 [3], the indoor thermal environment design and thermostat settings in the vast majority of buildings with mechanical systems rely on air temperature control values derived from the existing predicted mean value (PMV)

DOI: 10.1201/9781003371540-3

model. PMV is the most commonly used metric for assessing thermal comfort levels in a mechanically controlled environment. PMV is an indicator that predicts the mean value of a set of occupants' thermal sensation votes. The PMV model takes into account two human-related elements, the user's clothing insulation and metabolic rate, as well as environmental parameters such as temperature, air velocity, mean radiant temperature, and relative humidity.

Recent research have revealed various shortcomings of the PMV model when used in real-world scenarios. Firstly, because the model was created to estimate the average level of comfort for a large group of users, it has a low predictive accuracy when applied to a small sample of users. As well as, for the PMV model it is sometimes difficult to determine the exact value of the input variables in real-world circumstances. For example, throughout the day, the metabolic rate can fluctuate. Additionally, in a real-world setting, clothing insulation may not be constant over time, resulting in inconsistencies in PMV measurement. In general, these models, however, don't account for the complexity of human thermoregulation or the sufficiency of the thermal comfort offered; instead, they just show how the environment affects a person's thermal comfort. Furthermore, they disregard factors such as psychophysics, gender, age, and other physiological, psychological, cultural, and social settings that are known to influence how comfortable people feel in their surroundings [9,23]. As a result, they fail to provide optimal thermal comfort in practice [11,19].

Furthermore, different occupants may have distinct subjective responses when all other factors are equivalent. The scientific community has examined thermal comfort from the perspective of the individual and his or her perception of the environment, as thermal comfort is intimately tied to behavioral, physiological, and psychological aspects and hence varies between individuals [19].

In our previous research [20], we proposed a thermal comfort provision method based on environmental thermal sensation in four hot thermal environments. Since thermal comfort is a subjective psychological sensation and thermoregulation results in observable physiological changes [29], it would be more effective to provide thermal comfort based on a person's physiological signals and subjective responses. In this research, we focus on predicting personalized thermal comfort from empirically collected data in various work conditions: i.e., reading, typewriting, and gymnastics, focusing on hot thermal conditions in accordance with the ASHRAE scale: normal, slightly warm, warm, and hot thermal environments and evaluated subjective thermal responses on very hot, hot, warm, slighly warm, neutral, fresh, and cool scale. We present a thermal comfort providing approach using heart rate variability (HRV) data from simple wristwatch-like device equipped with various sensors to collect autonomic nervous system activity data. In this study, we collected data from 33 participants' 10 days data to evaluate the individuals' thermal comfort focusing on hot environment. During the experiment, participants reported their subjective thermal sensation states every five minutes using a thermal assessment logging application that we designed and placed on a smart tablet. We compared the environmental PMV thermal comfort prediction with subjective thermal

assessment and found that almost 74% personal assessment did not match with PMV environmental thermal prediction.

As well, in this chapter, we compared machine learning algorithms KNN, ET, LightGBM prediction performance with CNN prediction performance based on the person's HRV indices to predict the subjective thermal sensation sates. We checked the models' performance with low-granularity easily accessible data (e.g., only heart rate, accelerometers, skin temperature) but our investigation shows that only heart rate data with other low-granularity signal data cannot perform well for predicting thermal comfort labels hence the accuracy is only 56% in CNN model. On the other hand, the model performs good while several HRV indices were used as input to machine learning models as well as for the CNN model with HRV signals to anticipate users' personalized thermal sensation, providing an accuracy of 97.6%.

The rest of this chapter proceeds as follows: first, Section 2.2 begins by reviewing the related literature on estimating thermal sensation, comfort, and preference. Section 2.3 explains the methodology of this research, which includes data collection process, collected data overview, difference in PMV and individual thermal assessment, feature extraction process, and model development details. Section 2.4 presents the results of the prediction of different thermal sensations and classification methods with discussions. The conclusions drawn are presented with some future work points in Section 2.5.

## 2.2 BACKGROUND: THERMAL SENSATION, COMFORT AND PREFERENCE

It is challenging to provide a single definition for the concept of 'thermal comfort' since it is a phrase that can refer to a variety of subjective sensations and is influenced by all aspects that affect the thermal condition that an occupant experiences. All conditions under which a person would not choose a different environment are frequently referred to as human thermal comfort [40]. An additional definition of thermal comfort is given by American standard ASHRAE 55 [7], which characterizes it as a subjective term related to physical and psychological well-being with the environment. Because each person is unique, this word is typically used to describe a set of ideal conditions, for which the majority of a group of people can feel comfortable in their surroundings [13].

The term thermal comfort refers to every element that affects how heat is exchanged between the human body and its surroundings. This allows us to distinguish between factors related to the human body, such as age, gender, weight, metabolic rate, type of activity, etc.; factors related to clothing, such as thermal resistance, material structure, and number of layers; and factors related to the environment, such as air temperature, velocity, humidity, and pressure [12,13]. A personal thermal comfort model's main benefit is its ability to self-learn and update to suit a person with a data-driven approach, leading to improved prediction power.

By inputting various inputs into machine learning algorithms, numerous recent studies have built personal thermal comfort models. (1) Environmental information, (2) occupant behavior, and (3) physiological signals are the three main kinds

of variables. The classification of occupants' personal thermal comfort using temperature and humidity sensors was done using a data-driven approach with the indoor environment [17]. The second method is to observe how occupants behave, such as modifying thermostats [22] or personal heating/cooling device settings [35], in order to infer their level of comfort and preference with regard to the temperature. In addition to behavior-tracking, physiological markers including skin temperature [10,44], heart rate variability [32], electroencephalogram (EEG) [45], skin conductance [16], and accelerometry [39] also demonstrate a substantial link with human thermal feeling and comfort. Personal thermal sensation models were created by Sim et al. [43] based on wrist skin temperature readings from wearable sensors. By combining environmental, physiological, and behavioral data from the occupants, a "personalized" model can be created [26]. Other recent attempts [4,21] combined ambient sensors (such as temperature and air speed) with commercial wearable sensors to anticipate each individual occupant's comfort.

Although all of the research discussed above asserted improved prediction accuracy compared to traditional PMV and adaptive models, we highlight a few significant flaws or restrictions in those studies. In steady-state short-term lab testing, the dynamics of thermal comfort among many daily activities and their interactions cannot be properly recorded. Studies conducted under steady-state circumstances were unable to record human activity or mobility. Personal thermal comfort models created under realistic settings may be technically possible, but they may also be inaccurate.

Previous studies using wearable sensors frequently used readily available, inexpensive commercial sensors. Although the manufacturers claimed that the built-in sensors were accurate and reliable, it is unknown how well these sensors operated when worn. The manufacture specification was typically based on laboratory validation in a static setting, which could be very different when end users employed the sensors. For instance, a wristband like the Empatica E4 (Empatica Inc., USA) wristband [27] be reliable when there are less motions, like when sleeping and sitting at a table.

In this study, we developed personal thermal comfort models using lab-grade, wearable sensors that continuously analyze physiological inputs. We propose using heart rate variability (HRV) to discretely characterize individuals' thermal comfort state. HRV represents the time difference between two consecutive heartbeats. Heartbeat intervals (also known as the R–R intervals) are not periodic. Instead, the time between two successive R–R intervals changes from heartbeat to heartbeat. This variance, however, is not random; rather, it varies according to complicated extrinsic protocols placed on the heart [36]. HRV is also associated with homeostasis, which is the human body's ability to maintain optimal circumstances despite changing environmental stressors [37]. The hypothalamus in the human brain controls several mechanisms to enhance or decrease energy production in order to restore the body's core temperature. The parasympathetic nervous system (PNS) and the sympathetic nervous system (SNS) work together to keep the body in

balance (SNS). The two systems have opposite effects on the heart rate: the SNS makes the heart beat faster, while the PNS slows it down [38].

Since thermal comfort is a personal subjective assessment of the satisfaction of the mind with the thermal environment and that thermal changes in the environment affect homeostasis, which in turn affects HRV [8], we consider that thermal comfort state could be predicted more accurately using HRV. Thus, in this study, we evaluated subjective HRV indices under different work conditions and different hot thermal environments in order to classify the thermal comfort state of individuals in hot environment by using a simple wristband E4 empatica, which is a medical-grade wearable device that offers real-time physiological data.

## 2.3 METHODS

In this section, we describe the data collection procedure, data overview, differences between PMV and individual thermal assessment, physiological metrics used in this research, feature extraction, and model building process elaborately.

### 2.3.1 Data Collection

This section provides an overview of the data collection protocol, wearable sensors, participants, data collection process, and tools used for the experiment. Each participant gave informed consent to the processing of their data, which was obtained with the approval of the local ethics committee.

#### *2.3.1.1 Data Collection Protocol*

The data collection protocol designed for this experiment focuses on collecting data on hot thermal environments (neutral to hot environmental thermal states) under different activities (Figure 2.1). In a single data collection experiment, each participant experienced eight different experimental session conditions. Table 2.1, presents each experiment session condition elaborately. The experiment session conditions are focused on different work environments, such as reading, typing, and gymnastics with a focus on hot environments and settings in accordance with the ASHRAE scale. We have set these activities in real-world circumstances. For example, elderly people reading/watching television at home will be associated with reading activities, office work classroom study will be aligned with reading and typing activities, and factory/outdoor labor requiring higher effort will be aligned with heavy work activities like radio gymnastics (Figure 2.1).

Each session was planned with a specific activity and various humidity and temperature levels. For instance, gymnastics activities were recorded in both a hot condition (temperature 32°C and humidity 80%) and a warm state (temperature was 25°C and humidity 60%). In addition, reading and type writing activities were also recorded in varied temperature and humidity states. The duration of gymnastics activities was 10 minutes whereas other activities were 15 minutes. Participants took

TABLE 2.1 Data Collection States for a Single Experiment

| Experiment Session Conditions | Task | Temperature (°C) | Humidity (%) | Duration (minutes) |
|---|---|---|---|---|
| 1 | Radio gymnastics | 32 | 80 | 10 |
| 2 | Radio gymnastics | 25 | 60 | 10 |
| 3 | Reading | 25 | 60 | 15 |
| 4 | Reading | 32 | 80 | 15 |
| 5 | Reading | 27 | 60 | 15 |
| 6 | Reading | 32 | 80 | 15 |
| 7 | Typewriting | 32 | 80 | 15 |
| 8 | Typewriting | 27 | 60 | 15 |

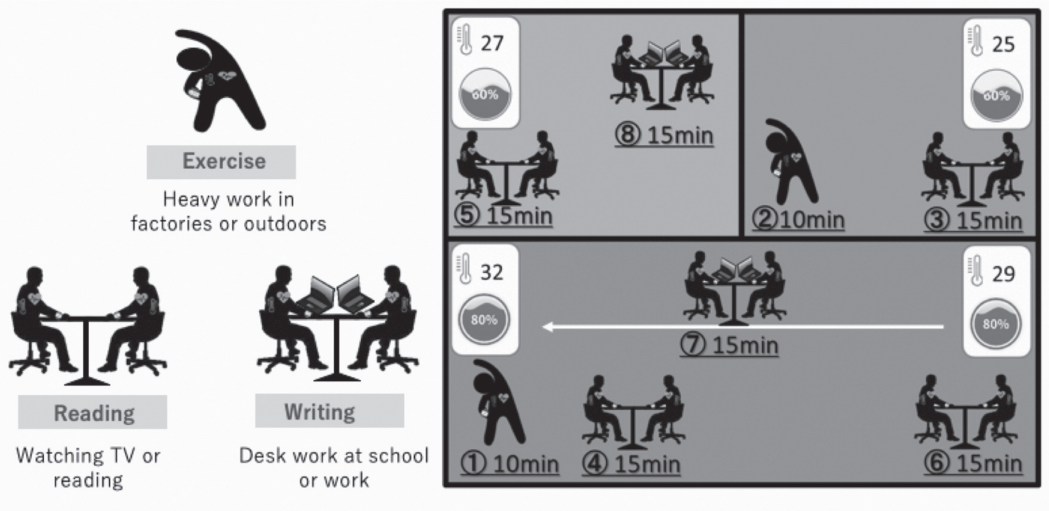


Figure 2.1 Experiment outline; data collection under different activities in different temperatures.

a 5-minute break after completing the gymnastics activities, which were recorded in hot temperatures (32°C/humidity 80%) and (temperature was 25°C/humidity 60%), so that the heavy activity in hot temperatures and humidity conditions did not affect the following experiment.

#### 2.3.1.2 *Wearable Sensors*

Participants were requested to wear Empatica E4 wristbands[1], it is a wristband that looks like a watch and contains numerous sensors, including an Electrodermal activity (EDA) monitor sensor, a photoplethysmography (PPG) sensor (which measures the Blood Volume Pulse (BVP), which is a metric that may be used to determine heart rate variability to assess sympathetic nervous system activity and heart rate simultaneously at the same time), and a three-axis accelerometer (ACC),

and an optical thermometer. At a sampling rate of 4 Hz, EDA shows how the skin's electrical properties are constantly changing. Increased skin conductivity is caused by an increase in the level of sweating. The PPG sensor, which measures the BVP at a frequency of 64 Hz, can be used to determine the IBI and HRV. Under seated rest, paced breathing, and recovery conditions, the Empatica E4 wrist band [28] accurately measures HRV. Thus, the E4 is outfitted with sensors that are designed to collect high-quality data [27].

#### 2.3.1.3 *Participants and Procedure*

Data was collected from a total of 33 participants, whose ages ranged from 22 to 50 years old (10 women, 23 men). The individuals who participated were given specific instructions on how to do a specified task while they were inside in a temperature-controlled environment. For this experiment, data were collected for 10 days. We made adjustments to the temperature and humidity at the time of data collection for each activity. The continuous pulse intervals of 33 adult males and females were measured in three different work situations involving reading, typing, and radio gymnastics under varying environmental conditions of temperature and humidity. During the experiment, participants wore the E4 Empatica wristband, which was connected with an android smartphone application named E4 real time via Bluetooth signal (Figure 2.2). Participants uploaded the data to the cloud server of E4 connect after each session ended.

For subjective evaluation, we developed a separate subjective thermal assessment logging application which was installed in a smart tablet and participants recorded their personal thermal sensation states in each 5 minutes during the experiment (Figure 2.3). The date and thermal comfort are recorded each time the user touches an icon. In the application, there is a timer sets which gives reminder to participants to record their personal assessment in every 5 minutes.

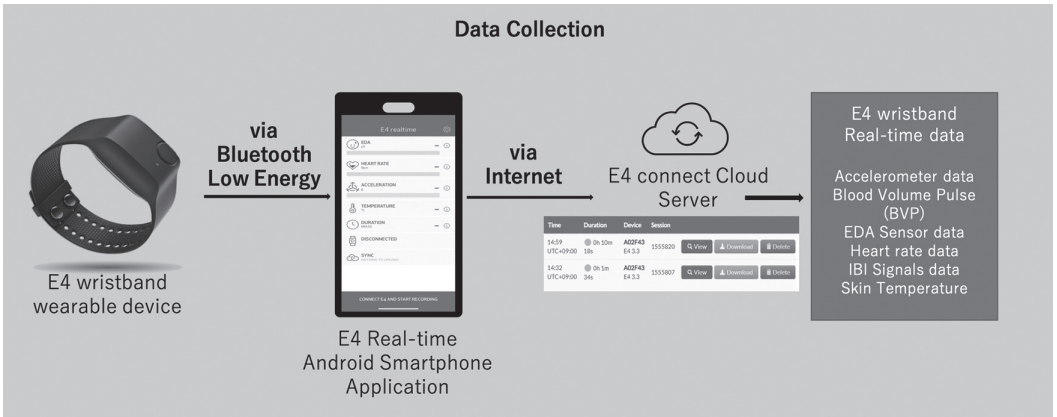


Figure 2.2 Overview of the data collection process.